

# Granular gases of rough spheres: velocity, rotation and collision statistics from in-situ measurements, optical data and simulations

Kirsten Harth<sup>1,2</sup>, Torsten Trittel<sup>1,2</sup>, Mahdieh Mohammadi<sup>1,2</sup>, Dmitry Puzyrev<sup>2,3</sup>, Mohammad Enezz<sup>1</sup>, Raul Cruz Hidalgo<sup>4</sup>, and Ralf Stannarius<sup>1,2,3</sup>

<sup>1</sup>Dept. of Engineering, Brandenburg University of Applied Science, Brandenburg an der Havel, Germany

<sup>2</sup>MARS, Otto von Guericke University Magdeburg, Magdeburg, Germany

<sup>3</sup>MTRM, Otto von Guericke University Magdeburg, Magdeburg, Germany

<sup>4</sup>Department of Physics and Applied Mathematics, Universidad de Navarra, Pamplona, Spain

**Abstract.** Granular gases are not only of interest in fundamental physics, but they can also serve as a test ensemble for the validity of collision models employed in (loose) granular matter. The theoretical literature mainly addresses spheres under ideal conditions and simulations allow full access to all particle parameters, but experiments cannot fulfill these idealizations. We investigate granular gases of soft, rough spheres by combining microgravity experiments and adjusted simulations. We introduce Smart Particles with embedded autarkic micro-sensors for in-situ measurements of rotation rates and accelerations. Additionally, we extract 3D positions, translations and orientations of the particles from stereoscopic video data using Machine-Learning based algorithms. We address the partition of kinetic energy between the degrees of freedom, the angular and translational velocity as well as collision statistics. A simulation is adjusted to experiment parameters, showing good agreement of translational motion, but qualitative differences in the decay of rotational kinetic energy.

## 1 Introduction

Granular gases, which represent ensembles of rarely interacting macroscopic particles, occur in many situations in nature and technology. While the analysis of collision and ensemble properties of this rather simple many-body system is of profound interest in statistical physics, it can also improve our models of denser flowing granular materials by allowing a quantitative, particle- and ensemble-based assessment of simulations against experiments. Due to frictional collisions, both translational and rotational degrees of freedom are always excited in a realistic granular gas. Theory and simulations in the literature almost exclusively address granular gases of spherical grains, often under idealized initial and boundary conditions and with rather simple contact models, while situations occurring in nature are usually more complex. Ground lab experiments mostly address two-dimensional layers affected by frequent contacts with the container, or require strong forcing to counteract sedimentation. For experiments in three dimensions (3D), micro-gravity ( $\mu g$ ) is needed, thus they are still scarce.

The first 3D  $\mu g$  experiments with spherical grains in vibrating containers displayed dynamic clustering [1]. Yet, translational velocity distributions have not been measured [2] and particle rotations have not been analyzed until recently [3] for spheres due to experimental complications. These aspects motivated studies of granular gases of more complex shaped bodies, like rods [4–10] and flattened ellipsoids [11]. In these cases, there are

two kinds of rotational degree of freedom: Those which are excited even without friction during collisions, due to an asymmetry in the particle shapes, and exclusively frictionally excited ones. For cylindrical rods, the former are the rotations around the short axes, which have been reconstructed from stereoscopic videos in 3D granular gases [5, 7–10]. These degrees of freedom have substantially lower kinetic energy than the translational ones in vibration-excited granular gases [4], and still slightly less during the periods of granular cooling observed in previous experiments [7, 8, 10]. The purely friction-coupled rotations around the long rod axis were hard to observe, only a qualitative assessment of a kinetic energy roughly one order of magnitude lower than the other degrees of freedom was made in experiments [8]. An increasing fraction of rotational energy during granular cooling was predicted in simulations [10].

A second aspect is the energy decay law in itself. The scaling of the energy (*'granular cooling'*) originally derived by Haff [12],

$$E(t) = E(0)/(1 + t/\tau_H)^2, \quad (1)$$

is robust across different experimental situations [2, 3, 8, 10, 11, 13], despite violations of several model assumptions such as spatial homogeneity. However, the predicted characteristic time scale  $\tau_H$  is usually longer than experimentally measured [2, 7, 8, 10]. It depends on the number of effective degrees of freedom, the mean free path length and thus the filling fraction, the particle shape, and the velocity and energy distribution in the ensemble; see e.g.

Ref. [14]. Numerical simulations with matching geometries and parameters, e. g. for rods in Refs. [10, 15, 16], may help to elucidate the impact of ensemble and collision parameters. Quantitative experiments are needed for the calibration and evaluation of models. Inversely, validated models can help identify and analyze experimental results in view of theoretical models.

This motivated the present study of granular gases of centimeter-sized frictional spheres. We measured rotations and translations of the particles using a combination of optical stereoscopic videos with properly marked particles, and employed Smart Particles (individual grains with autarkic embedded micro-sensors) for in situ acceleration and angular velocity data. Microgravity experiments were accompanied by the adjustment, validation and application of a simulation model using soft, frictional spheres. In drop tower experiments, we investigated granular cooling, and permanent excitation was applied in parabolic flights. Here, we present an overview of the methods employed and first results. Details will be published elsewhere.

## 2 Methods

Granular gases consisting of 3.5 cm diameter rubber spheres were observed in microgravity at the ZARM drop tower Bremen 4.7 s  $\mu g$ , with a remaining acceleration  $10^{-6} g$ , Sec. 3.1) and during parabolic flights (A310 Zero-g, 22 s  $\mu g$ , remaining acceleration ( $g$ -jitter) up to 0.1  $g$ , Sec. 3.3). Up to 300 particles were placed in a  $30 \times 30 \times 40$  cm<sup>3</sup> cuboid container, shown in Fig. 1. The upper and lower walls can be actuated with controlled frequency and amplitude. Data were recorded by two Go-Pro Hero Ribcage cameras at up to 240 frames per second and  $1920 \times 1080$  pixel<sup>2</sup>. Differently colored hemispheres and markings on the balls allow for identification and detection of their orientations. We use a machine learning-assisted detection algorithm for the positions, similar to that used for rodlike particles [9]. In the present paper, we study two types of particles: First, rubber spheres of 22.4 g mass and a moment of inertia of 27.4 g cm<sup>2</sup>, filled with a central plastic sphere [3] in all optical data analyzed in Sec. 3.1. Their normal coefficient of restitution measured for sphere-wall collisions is 0.9. Second, we mixed rubber beads with 30 Smart Particles in the parabolic flight experiments. These are lighter,  $m = 17.5$  g, 3.5 cm in diameter custom-designed 3D-printed particles of foamable colored TPU with smaller coefficient of restitution for wall collisions. Each of them hosts an autarkic IMU Sensor boards (221e MUSE inertial config), see Fig. 1 (right). Power was supplied by 3 AG5 batteries. Accelerations and angular velocities were recorded at rates of 800 Hz or 1600 Hz. First results are shown in Sec. 3.3. In-situ measurements using acceleration and gyroscope sensors embedded in individual grains have been employed in granular impact and silo discharge before [17–19].

Numerical simulations were performed using a combined GPU-CPU based Discrete Element Method (DEM) based on earlier studies of rough spheres [20] and rods [10, 15, 16, 21]. We used a Hertzian type model, scaling with the overlap distance of spheres at the moment of collision

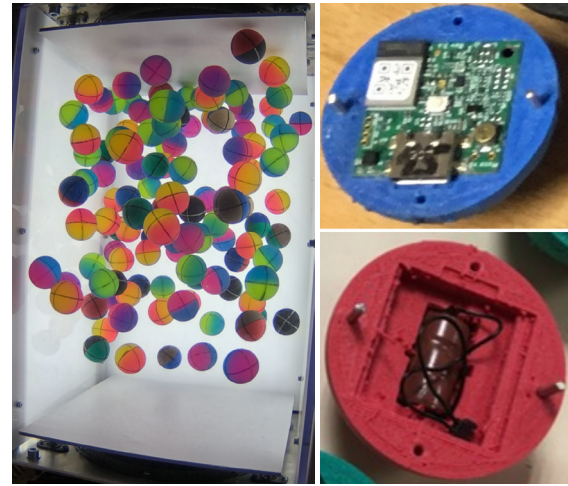


**Figure 1.** Left: Granular gas of 120 marked 3.5 cm diameter spheres (including 30 smart particles, non-translucent) in our parabolic flight experiment. The particle number density inhomogeneity is due to residual accelerations. Right: The two hemispheres of a smart particle with sensor board and batteries.

for the normal contact force. The Young modulus was set to 50 MPa. Tangential forces were modeled using a constant effective friction coefficient.

## 3 Results

### 3.1 Optical measurements: Granular cooling

The rotations and translations in two drop tower experiments with  $N = 57$  (filling fraction 3.6%) and  $N = 88$  (filling fraction 5.5%) particles were evaluated manually from a 2D projection [3], where two translational and two rotational degrees of freedom were accessible. The particles were subjected to vibrating side walls for 2 seconds followed by the cooling phase in microgravity. Experiments with higher fill fraction are under evaluation and the results will be published elsewhere. The symbols in Figure 2 (top) show the decay of the rotational and translational kinetic energies per particle. Despite the inhomogeneous initial state, particularly of the translational velocities typical for vibrational excitation [22], the decay follows Haff's scaling Eq. (1) with  $\tau_H \approx 1.2$  s in both experiments. This is surprising as it indicates a similar amount of dissipation in the two experiment runs. By counting the collisions of particles with the walls and between the particles in both experiments after start of cooling, both display a nearly identical increase with  $N_{\text{part}} \approx 3.65 \ln(1 + t/1.2 \text{ s})$  and  $N_{\text{wall}} \approx 2.15 \ln(1 + t/1.2 \text{ s})$ , consistent with equal Haff times. In both experiments, the rotational energies  $E_R$  are less excited than the translational ones  $E_T$  with a ratio of  $E_R/E_T \approx 0.6 \dots 0.65$ , with strong statistical fluctuations. The translational and angular velocity distributions are roughly Maxwellian, yet display a slight overpopulation of fast particles, for details see Ref. [3]. Better statistics are needed for a more accurate quantification.

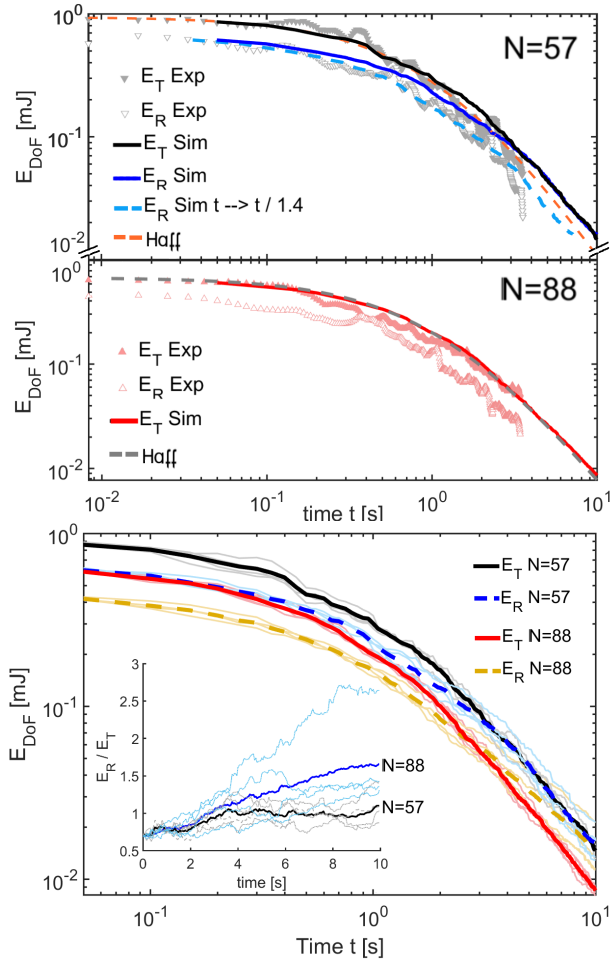


**Figure 2.** Granular cooling,  $N = 57$  or  $N = 88$  spheres: top: experimental data (symbols) for rotational and translational energy per particle compared to our simulations (solid lines), or orange resp. grey dashes: Fit to Eqn. (1) with  $\tau = 1.2 \pm 0.08$  s,  $E_0 = 0.94$  mJ,  $N = 57$  and  $E_0 = 0.67$  mJ,  $N = 88$ . Bottom: simulation result as average of 4 individual runs (light shaded lines). Rotation energies (cyan dashes) decay more slowly than the experimental ones. The inset shows the ratio of rotational to translational kinetic energy.

### 3.2 Simulation

Motivated by the experiment, we simulated the granular cooling of  $N = 88$  and  $N = 57$  spheres in a  $30 \times 30 \times 40$  cm<sup>3</sup> container. We considered cooling from a random state of initial mean rotational and translational kinetic energies equal to the experiment, starting with globally uniform particle and (rotational) velocity distributions. Data were averaged over 4 realizations with slightly different initial data sets; see Fig. 2 (bottom). We achieved an identical decay rate of the translational energy as in the experiment by adjusting the effective friction coefficient to 0.5 and the normal coefficient of restitution to 0.8; see Fig. 2 (top). This set of parameters worked well for the translational energies in both experiments. However, the rotational kinetic energy displayed a qualitatively different behavior, see Fig. 2, which could not be adjusted satisfactorily by tuning the elastic modulus, restitution and friction coef-

ficients. The decay still approximately follows Eq. (1), but with larger  $\tau_H$ , i.e. with less effective dissipation. In Fig. 2 (top), we exemplarily rescaled the time for the simulated rotational energy (blue dots) for  $N = 57$  with a factor of  $1/1.4$  (light blue dashes) to roughly match the experimental data. The energy ratio  $E_R/E_T$  (inset of Fig. 2 bottom) shows an initially increasing trend for both data sets, where saturation is not reached for  $N = 88$  particles within the simulation time of 10 s. This is a clear contradiction to the experiments, where no significant trend of the ratio  $E_R/E_T$  was observed. An increasing ratio corresponds to an unbalanced energy transfer from translational to rotational degrees of freedom, leading to increasing dominance of rotational motion over translations. This would have the drastic consequence of a granular gas of constantly rotating particles in the limit of practically vanishing translational velocity. Preliminary simulations with larger particle numbers show that decreasing the value of the friction coefficient can lead to an earlier and stronger dominance of rotations over translations [23]. This is inconsistent with Haff’s scaling of the overall energy decay.

One qualitative difference between experiment and simulation is the initial state. Another difference are deviations in the number of particle-wall and particle-particle collisions: While the number of collisions in all cases increases proportional to  $\ln(1 + t/\tau_H)$ , we find a significantly larger fraction of  $N_{part,88}/N_{wall,88} \approx 2.7$  for  $N = 88$  compared to  $N_{part,57}/N_{wall,57} \approx 1.8$  for  $N = 57$  and to  $N_{part}/N_{wall} \approx 1.7$  in both experiments. The difference between these collision types in the simulation could be a possible reason for the observed discrepancies.

### 3.3 Smart Particles: Rotations and collisions

Reliable access in optical measurements to both rotational velocities and collision rates is hard and time consuming, in particular in denser agitated systems with frequent particle overlaps and collisions. The discrepancy between our simulation and experiment indicates the need of high-quality, easily accessible information. We performed a first series of experiments during a parabolic flight and extracted angular velocities and accelerations in a particle fixed coordinate system from in-situ sensors, see Fig. 3 (top). Collisions are easily identified by peaks in the absolute acceleration between  $\approx (2 \dots > 50)g$  (clipped in the image). As expected, rotation rates are roughly constant between collisions due to the conservation of angular momentum. When we analyze a parabola where residual velocities due to the remaining accelerations ( $g$ -jitter) are small compared the particle velocities, the distribution of the times  $\Delta t$  between consecutive collisions follows typical decay curves seen in Fig. 3 (bottom).

## 4 Conclusion

We have successfully implemented an in-situ measurement with Smart Particles in a granular gas of spheres in a microgravity experiment, combined and validated with stereoscopic optical techniques. This provides direct, precise access to collisions and angular velocities, otherwise

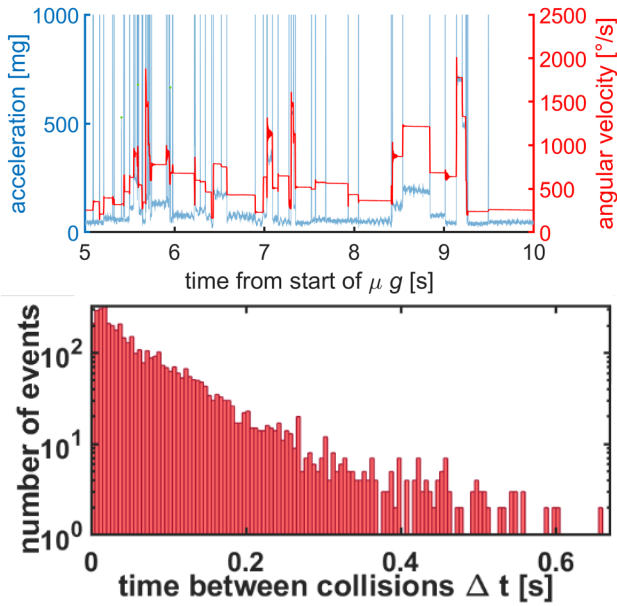


**Figure 3.** Smart particles: In-situ measurements in a granular gas of 120 spheres under permanent vibrational excitation during micro-gravity in a parabolic flight, top: absolute rotational velocity and acceleration of an exemplary particle (selection). bottom: Distribution  $P(\Delta t \geq t)$  of the interval  $\Delta t$  between collisions of 28 Smart Particles during seconds 5...20 in one parabola

hard to access. As the particles are marked, rotations and translations could be extracted from stereoscopic video data. We showed that the cooling of frictional spheres follows Haff's scaling, but with shorter time scale than predicted by theory. Contrary to expectations from earlier simulations [24], the experimental energy ratio reaches a constant value  $E_R/E_T < 1$ . A permanently driven ensemble displays a characteristic distribution  $P(\Delta t \geq t)$  of the time intervals between collisions. Ideally, with a uniform speed of all particles, it would be exponential. By adjusting the effective friction and restitution coefficients, we achieved a match between our simulations (based on a Hertzian contacts) to the energy decay of translations, whereas the rotations display a longer decay time, causing an increase of the share of rotational energy with time in contrast to experiments. The reason for this discrepancy may lie in the different ensemble behavior in simulation and experiment, or even in an inappropriate contact model. Our novel technique opens the path toward quantitative in-situ studies in granular gases beyond the small-ensemble and dilute limits, including realistic, quantitatively matching simulations.

## Acknowledgments

We thank the German Aerospace Center (DLR) for funding by grants KORDYGA (50WM2242), JACKS (50WM2340), EVA (50WM2048/50WK2348). R. C. Hidalgo acknowledges financial support of the Spanish Government in grant No. PID2023-146422NB-I00 (MICIU/AEI/10.13039/501100011033). We thank ZARM, Novespace and DLR for their support of the campaigns.

## References

- [1] E. Falcon, R. Wunenburger, P. Evesque, S. Fauve, C. Chabot, Y. Garrabos, D. Beysens, *Phys. Rev. Lett.* **83**, 440 (1999).
- [2] P. Yu, M. Schroeter, M. Sperl, *Phys. Rev. Lett.* **124**, 208007 (2020).
- [3] D. Puzyrev, T. Trittel, K. Harth, R. Stannarius, *npj microgravity* **10**, 36 (2024).
- [4] K. Harth, U. Kornek, T. Trittel, U. Strachauer, S. Höme, K. Will, R. Stannarius, *Phys. Rev. Lett.* **110**, 144102 (2013).
- [5] K. Harth, T. Trittel, U. Kornek, S. Höme, K. Will, U. Strachauer, R. Stannarius, *AIP Conference Proceedings* **1542**, 807 (2013).
- [6] K. Harth, T. Trittel, K. May, S. Wegner, R. Stannarius, *Adv. Space Res.* **55**, 1901 (2015).
- [7] K. Harth, T. Trittel, S. Wegner, R. Stannarius, *Powders & Grains in press* (2017).
- [8] K. Harth, T. Trittel, S. Wegner, R. Stannarius, *Phys. Rev. Lett.* **120**, 214301 (2018).
- [9] D. Puzyrev, K. Harth, T. Trittel, R. Stannarius, *Microgravity Sci. Technol.* **32**, 897 (2020).
- [10] D. Puzyrev, T. Trittel, K. Harth, R. Stannarius, *npj microgravity* **10**, 36 (2024).
- [11] S. Pitikaris, P. Bartz, P. Yu, S. Cristoforetti, M. Sperl, *NPJ Microgravity* **8**, 11 (2022).
- [12] P.K. Haff, *J. Fluid Mech.* **134**, 401 (1983).
- [13] C.C. Maaß, N. Isert, G. Maret, C.M. Aegerter, *Phys. Rev. Lett.* **100**, 248001 (2008).
- [14] F. Villemot, J. Talbot, *Granular Matter* **14**, 91 (2012).
- [15] T. Pongo, D. Puzyrev, K. Harth, R. Stannarius, R.C. Hidalgo, *EPJ Web of Conf.* **249**, 4003 (2021).
- [16] D. Puzyrev, D. Fischer, et al., *Scientific Reports* **11**, 10621 (2021).
- [17] E. Altshuler, H. Torres, A. Gonzalez-Pita, G. Sanchez-Colina, C. Perez-Penichet, S. Waitukaitis, R.C. Hidalgo, *Geophys. Res. Lett.* **41**, 3032 (2014).
- [18] S. Köstler, J. Zhao, C. Lyu, S. Völkel, K. Huang, *EPJ Web Conf.* **249**, 15007 (2021).
- [19] Y. Zhu, H. Yang, R. Li, Y. Zhang, Q. Chen, Y. Hua, Q. Sun, P. Kong, *Powder Technol.* **360**, 882 (2020).
- [20] R.C. Hidalgo, T. Kanzaki, F. Alonso-Marroquin, S. Luding, *AIP Conference Proceedings* **1542**, 169 (2013).
- [21] D. Puzyrev, R.C. Hidalgo, D. Fischer, K. Harth, T. Trittel, R. Stannarius, *EPJ Web of Conf.* **249**, 04004 (2021).
- [22] C. Yanpei, P. Evesque, M. Hou, C. Lecoutre, F. Palencia, Y. Garrabos, *J. Phys.* **327**, 012033 (2011).
- [23] M. Mohammadi, R.C. Hidalgo, T. Trittel, R. Stannarius, K. Harth, *Simulation of heating and cooling in a granular gas of soft rough spheres in microgravity*, *Proceedings of ESA PACs* (2024).
- [24] M. Huthmann, A. Zippelius, *Phys. Rev. E* **56**, R6275 (1997).